Analysis of Cutting Temperature of Drill Point

Analysis of Cutting Temperature of Drill Point

Koichi OGAWA,* Katsushige ADACHI,** Keizo SAKURAI**
Ralph NIBA**and Yoshinao TAKASHIMA*

(Received June 15, 1991)

The main objective of the present paper is to discuss cutting temperature of the drill point in low frequency vibratory drilling of stainless steel (SUS 304). Although many studies dealing with drill wear in conventional drilling have been presented, there has been hitherto no study dealing with cutting temperature of the drill point in low frequency vibratory drilling of SUS 304.

For this reason, cutting temperature in low frequency vibratory drilling of SUS 304 was selected as the subject of study, that is, cutting temperature in the drill face was measured by utilizing cobalt high speed steel drills brazed with sheathed thermocouples, and the experimental results were compared with those of conventional drilling. Futhermore, distribution of cutting temperature in the drill point was computed by the finite element method.

From this study, distribution of cutting temperature in the drill point was clarified.

1. Introduction

A large proportion of metal machining processes is covered by the process of hole making. As a result of this widespread use of drills, the automation of the drilling process is being vigorously pursued.However, problems such as extended drill life, efficient chip disposal, excellent hole finish and so on have to be realized to fully meet automation requirements.

Whereas the use of tough materials such as stainless steel, titanium alloys has been gaining ground, the effective drilling of these tough materials is marred by lots of limitations which have to be overcome. The drilling of these tough materials in particular is one of the difficult problems being faced by the metal machining industry. One of the problems confronted when drilling tough materials is poor chip disposal, thus, giving rise to an increase in cutting edge temperature. This drawback is attributed to the very low heat conductivity and the tendency for these materials to easily work harden. Another striking problem associated with the drilling of tough materials is the severe adherence of chips on the drill face thus, hampering the drilling action.

* Course of Instrument Science, College of Integrated Arts and Sciences.
** Faculty of Engineering, Osaka Sangyo University

Low frequency vibratory drilling is one of the drilling methods believed suited to drilling tough materials. Surprisingly so far, there has been very little research on this promising drilling method. The only prominent study on vibratory drilling in tough materials was reported by E. A Satel.

Considering the strategic importance of stainless steel, hole making in stainless steel (SUS 304) was taken up as the theme of study by the authors. Special attention is paid to the drill point temperature which has a direct bearing on the performance of a tool. In addition, cutting forces (thrust, torque) and tool wear are also given consideration. The correlation between cutting temperature and tool wear is looked into besides, the three dimensional heat conduction analysis of the cutting edge by the finite element method is undertaken to study the temperature distribution at the face and flank.

2. Experimental device and method

2. 1 Device

The experimental apparatus employed in this investigation is shown in Fig. 1. Low frequency vibration was applied to the drill in the axial direction with the aid of the hydraulic servo mechanism shown in the photograph in Fig. 1. The setup is such that, low frequency vibration (0～100Hz) is applied synchronously with the rotation of the drill in an axial direction. Cutting forces (thrust,torque) were measured with the aid of a Kistler piezo-electric dynamometer (model 9273) and the measured values were recorded and processed with a personal computer.

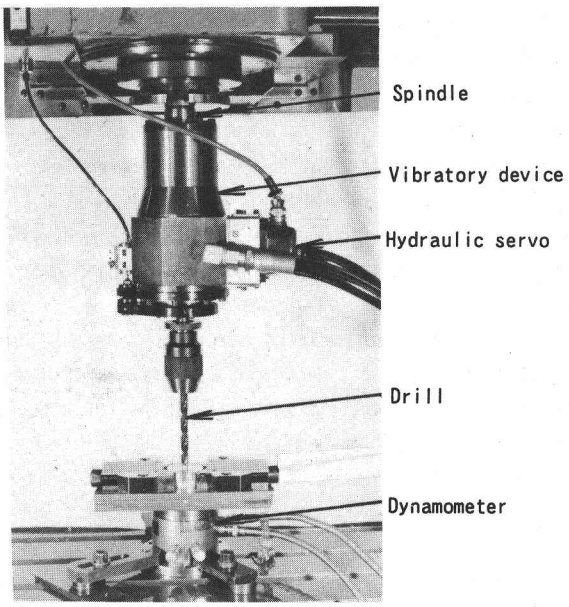

Fig. 1 Low frequency vibratory device

2. 2 Cutting temperature measurement

A sheathed thermocouple was employed to measure the cutting edge temperature. There are numerous research on cutting temperature but to the best of our knowledge there is none on drill face temperature measurement.

The method used in this study is really an originality in that, first of all, a hollow groove was created close to the margin and then a sheathed thermocouple was implanted in it, making sure one end of the thermocouple was on the face close to the flute and then the drilling action was performed. Fig. 2 shows the points where the sheathed thermocouple were inserted. It should be noted that the insertion was carried out at three different positions, on three different drills denoted C-1, C-2 and C-3 in the table below. Where r is the distance of the measured point (r=2.7mm, 3.5mm, 5.9mm) from the drill tip. The face temperature measuring setup is displayed in Fig. 3.

2. 3 Workpiece and drill

The workpiece used in this investigation was solution heat treated austenitic stainless steel plates of dimension (200×300×20). The heat treatment was performed at 1100°C for an hour after which the workpiece was reground. The drills used

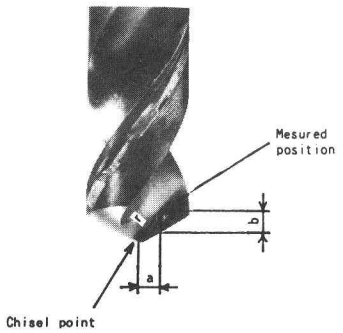

Drill	a(mm)	b(mm)	r(mm)
C-1	1.3	1.7	2.7
C-2	1.7	2.2	3.5
C-3	3.2	3.1	5.9

Fig. 2 Position of thermocouple on drill face

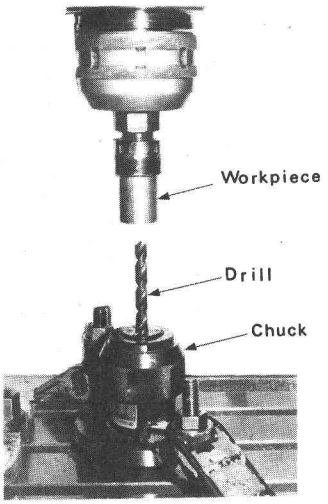

Fig. 3 Drill point temperature measurement setup

were cobalt high speed steel drills (JIS SKH56) of diameter 10mm. A model of the drill with an inserted thermocouple is shown in Fig. 4. In order to minimize variations,only drills from the same lot were used. A water soluble lubricant (JSIS W2-3) was employed and the rate of flow was held constant at 3.2 l/min.

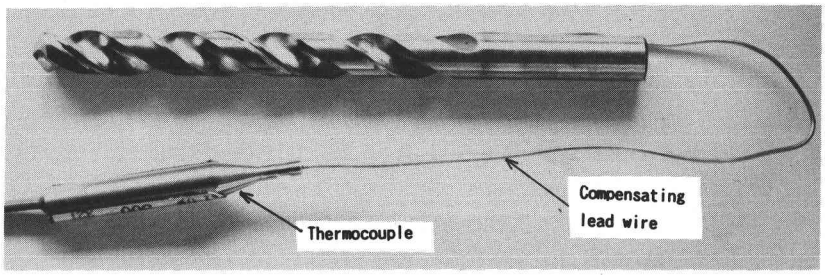

Fig. 4 Photograph of drill with inserted thermocouple

3. Results and discussion

3. 1 Cutting forces and tool wear

Cutting forces (thrust, torque) during low frequency vibratory drilling hereafter referred to as vibratory drilling are shown in the diagram in Fig. 5. For comparison, the thrust and torque forces during conventional drilling are also displayed.

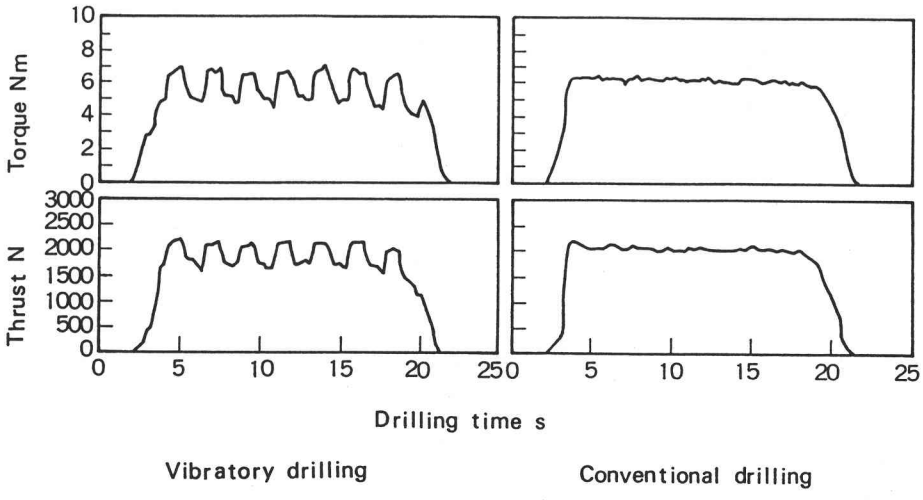

Drill dia. 10mm, Revolution 7.3S^{-1}, Feed rate 0.15mm/rev., Drilling depth 20mm, Frequency ratio 0.1cycle/rev, Oil cutting.

Fig. 5 Comparison of cutting forces (thrust, torque)

As it can be observed in the diagram, the thrust and torque in vibratory drilling fluctuate widely as a result of the periodic fluctuation of feed. Observation of the thrust and torque curves about 5s after penetration of the drill in the workpiece

reveal in the case of vibratory drilling, a thrust force of about 1600N～2050N, while the torque force is about 5.0Nm～6.6Nm. The static component of these forces that is the average of the periodic fluctuation, are thrust force of 1825N and torque force of 5.8 Nm. Whereas, the conventional drilling thrust and torque curves yield readings of 2000N and 6.3Nm respectively. A look at the curves in the diagram, reveal that thrust and torque forces for vibratory drilling are 23% and 27% lower than those in conventional drilling.

A look at the photographs of both drilling methods displayed in Fig. 6 reveal the absence of built-up edge on the face and just little wear on the chisel, while wear of the cutting edge of drills employed in the vibratory drilling tests is fairly uniform in nature whereas, considerable wear can be noticed on the outer corners of drills employed in conventional drilling tests. The wear of the cutting edges on the outer corners proceeds remarkably fast during conventional drilling leading to the accumulation of built-up edges on the chisel causing chips to pack easily in the hole thereby hastening tool failure.

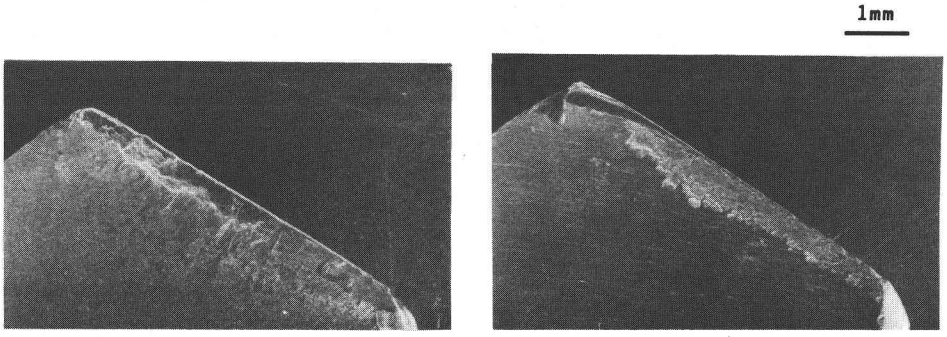

Drill dia. 10mm, Revolution 7.3 S^{-1}, Feed rate 0.15mm/rev., Drilling depth 20mm, Frequency ratio 0.1cycle/rev., Oil cutting

Fig. 6 Comparison of tool wear

From the viewpoint of tool wear and cutting forces, the above results reveal the superiority of vibratory drilling over conventional drilling. The main reasons for this superiority are the reduction in friction heat between the workpiece and tool as well as the curb in built-up edge formation during vibratory drilling. Wear of the cutting edges is believed to be influenced especially by friction heat.

3. 2 Cutting edge temperature

In the foregoing test, face temperature mesurement for both drilling methods were perfomed. Fig. 7 is a plot of distance from chisel point against temperature. Temperature readings at the face were taken at a drilling depth of 20mm at three different points from the chisel point.

As it can be seen in the diagram in Fig. 7 the face temperature for both drilling methods is higher near the chisel edge C-1 and margin C-3 than the central portion C-2. A close examination of the diagram also reveals that the face temperature near the chisel point and margin are lower for vibratory drilling than conventional

drilling.This is attributed to the lower heat dissipated near the chisel and margin during vibratory drilling.

Figure 8 shows the relationship between drilling depth and temperature. The diagram reveals that the face temperature near the chisel edge C-1 in vibratory drilling is 10～30°C lower than that for conventional drilling. It can also be observed that cutting temperature increases with depth. However,the temperature curve for vibratory drilling in particular is irregular in nature whereas that for conventional drilling is fairly linear.

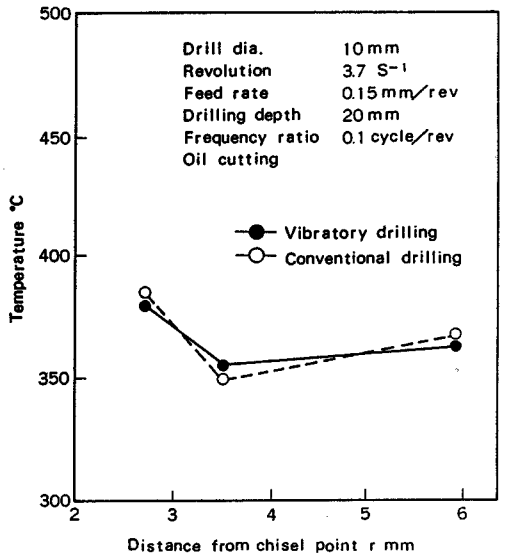

Fig. 7 Plot of cutting temperature versus distance of thermocouple from chisel point

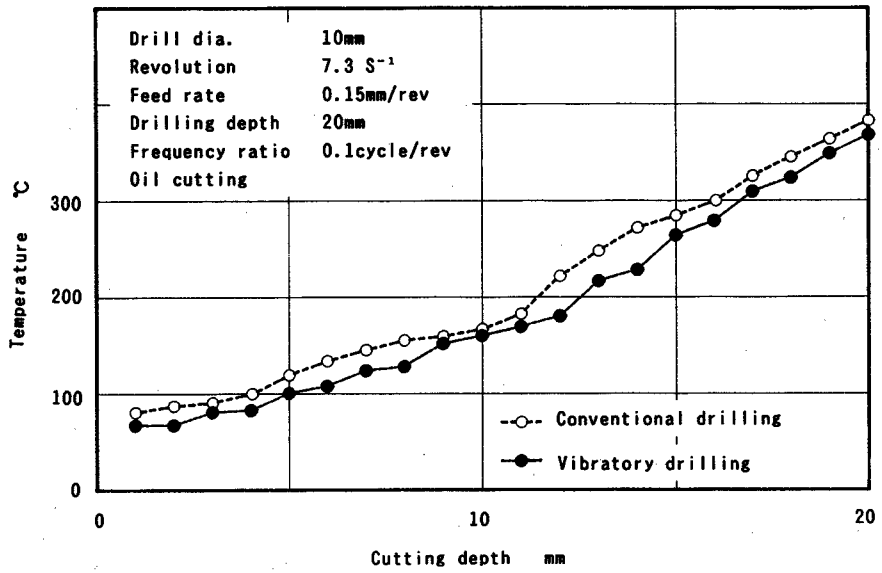

Fig. 8 Effect of cutting depth on cutting temperature

The irregular temperature curve obtained during vibratory drilling is believed to be due to the pulsating effect of the vibratory shocks on the cutting edge. While the drop in temperature can be attributed to improved coolant penetration as a result of the vibration enabling the coolant to reach the cutting edge thereby curbing wear of the cutting edges. The reduction in tool wear and cutting forces (static components) during vibratory drilling is in good agreement with this observation.

4. Analysis of cutting edge temperature by finite element analysis

As it was previously elaborated, the localized temperature at the drill face can be measured. However,the entire cutting edge temperature is exceptionally difficult to measure due to the three-dimensional geometry of the drill point. Finite element analysis is effective in tackling a task of this nature. Surprisingly, there is as yet no study incorporating the finite element method in drill cutting temperature analysis despite the conveniences it embodies.

Thus, the finite element method was employed by the authors to theoretically analyse the cutting edge temperature in conventional drilling. As previously pointed out, the theoretical analysis of the cutting edge temperature on a three-dimensional basis entails a lot of difficulties. As a result, in the foregoing analysis attention is paid to the case involving the formation of continuous chips, which is conventional drilling.

4. 1 Technique of drill point temperature analysis

The technique leading to an understanding of the drill face temperature distribution advanced by Shirai et al. entails the solving of unsteady state heat conduction equations to derive the final steady state temperature distribution. However, in a case involving the continous ejection of chips, the temperature distribution is thought to be unsteady due to heat dissipation from within the material. Thus, if initially after a fixed time has elapsed this technique is treated as a steady state problem it would be more practical from the viewpoint of reduced computation time. Thus, in the foregoing analysis, the ordinary differential equation for unsteady state heat conduction (equation 1) was solved using the finite element method.

$$\kappa \cdot \nabla^2 T + \dot{Q} - \rho c \frac{\partial T}{\partial t} = 0 \tag{1}$$

where T is the temperrature, t is the time, Q is the internal heat dissipation ratio, ρ, κ and c are respectively density, thermal conductivity and specific heat of the material.

Unlike the three dimensional cutting action of tool bits, the flow of heat along the cutting edge during the three dimensional cutting action of drills cannot be neglected. In addition, in the case of drills the flow of heat from chips to the drill has to be considered, viz, heat conduction and heat velocity boundary conditions have to be also given consideration. However, since it is impossible in a strict sense to derive

the heat distribution over an entire drill, equation (1) was idealized by finite element method in cases where provision for temperature T is given as a boundary condition for steady state heat conduction and the division of the drill point into elements was implemented. The temperature distribution in an element is depicted by equation (2).

$$T(x,y,z:t) = \sum_{i=1}^{n} N_i(x,y,z)\,\phi_i(t) \tag{2}$$

where N_i (x,y,z) is the shape function of the element; $\phi_i(t)$ is the temperature at node i at time t and n is the number of nodes in the element. A further idealization of equation (2) yields the finite element equation (3) given by

$$[K_{mn}]\ \{\phi_n\} = \{R_m\} + \{S_m\} \tag{3}$$

The computer program for three-dimensional heat conduction analysis by Yagawa et al. was used as reference.

4. 2 Finite element idealization

The drill has a twisted flute and since the drill point thins out toward the tip, it is extremely difficult to truly perform the three-dimensional idealization of the drill point, Thus, in this analysis the drill point was divided into surfaces or sections in a perpendicular directon to the drill axis and the various sections were assembled, creating a model as shown in Fig. 9. The idealized model is an isoparametric hexagon with each element having eight nodes. It is desirable for all the divided sections to have the same number of elements but since the drill point thins out toward the tip, reduction of the number of elements on each section was adopted. Furthermore, because the chisel cannot be associated with finite elements, the surface 0.1mm below the chisel was designated the first section and the surface 4. 9mm from the drill tip was divided into 15 sections (denoted A to P making altogether 16 sections). Next, each section was idealized into rectangular elements. The Z coordinate of each section is shown in Table 1. An idealized model is given in Fig. 10.

It should be mentioned that section L to section P lie on the same surface. An assembled model of section A to section L is depicted in Fig. 11, there are all together 2880 finite elements and 3542 nodes in this model. The finite element mesh diagrams of the drill face(a)and flank(b)at a point 3mm from the drill tip are shown in Fig. 12.

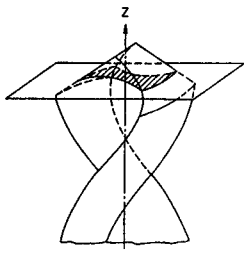

Fig. 9 Diagram showing sectioned surface perpendicular to drill axis

Table 1 Distance of sections from the chisel point in a plane perpendicular to the drill axis

Section	Z-coordinate (mm)	Section	Z-coordinate (mm)
A	0.1	I	2.4
B	0.3	J	2.7
C	0.6	K	3.0
D	0.9	L	3.3
E	1.2	M	3.7
F	1.5	N	4.1
G	1.8	O	4.5
H	2.1	P	4.9

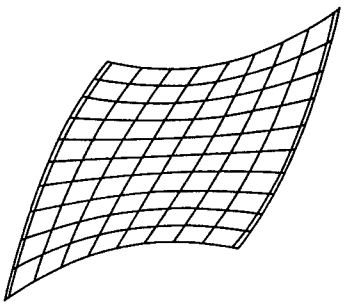

Fig. 10 Finite element idealization of section F (Total No. of nodes =121 ; elements=100)

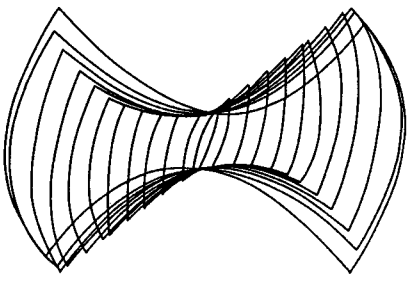

Fig. 11 An assembled model of section A~L

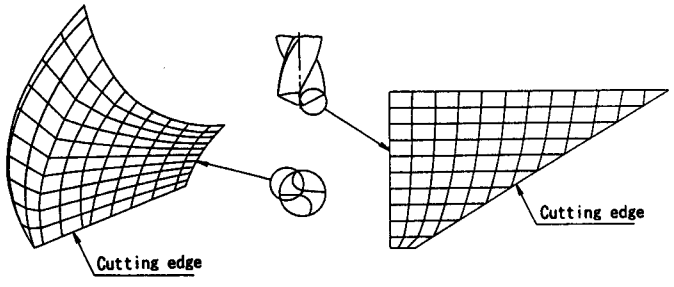

Fig. 12 Finite element idealization of drill flank and face

4. 3 Boundary conditions

The following procedure was used to apply the boundary conditions employed in the analysis. First of all, pre-recorded values of the face temperature from the face temperature experiment were recorded and then the chisel and margin temperature(maximum temperature)within each surface was held constant while all other boundary conditions were specified as radiation boundary conditions. The chisel and margin temperatures were measured by inserting sheathed thermocouples in the workpiece at the portions shown in the diagram in Fig. 13. Consideration was given to the temperature value used as boundary condition because of temperature differences at the various outer corners. Values for ς, c and $\varkappa$ used in the analysis, are respectively 7.82mg/m³, 0.536KJ/Kg • K and 42.6W/m • K.

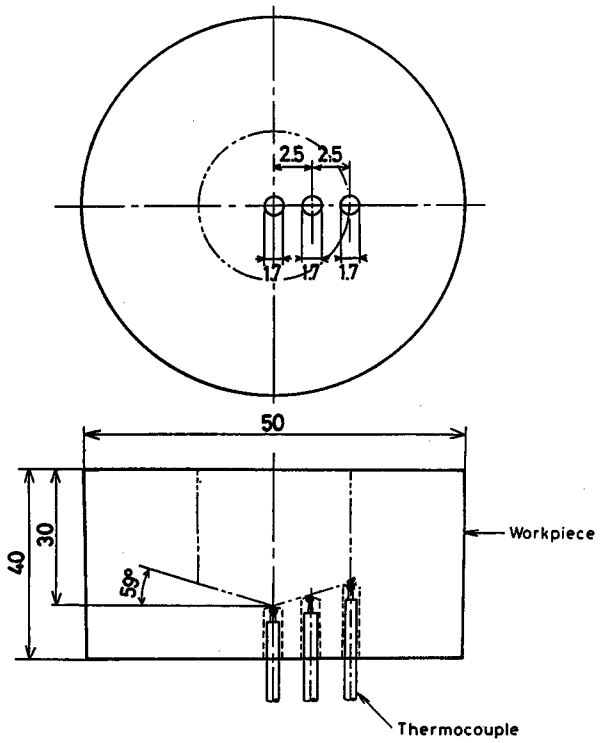

Fig. 13 Position of thermocouple in workpiece

4. 4 Results of numerical analysis and comparison with measured results

The calculated results of the isothermal temperature distribution within the drill face and flank are shown in the diagrams in Fig. 14 and 15. As was previously emphasized, readings were taken at a point 3mm from the drill tip. A look at the temperature slopes in the face temperature distribution diagram reveal the direction of chip flow while, the temperature slopes in the flank diagram leads to an understanding of the nature of heat generation at the chisel. Comparing these results with the measured values in the drill face reveal that the temperature difference with drill C-3 was 15°C,while the temperature difference with drills C-1 and C-2 was 8°C. That is, the numerical values are higher than measured values.

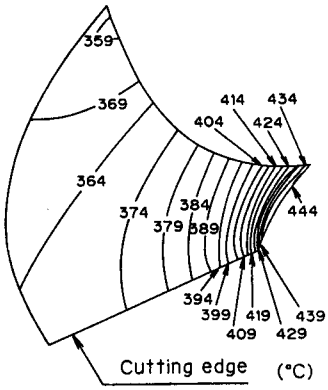

Fig. 14 Calculated values of flank temperature

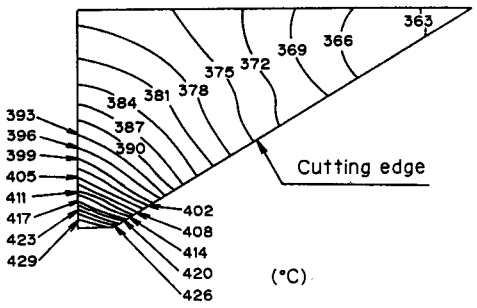

Fig. 15 Calculated values of face temperature

In the case of cutting temperature in vibratoy drilling where cutting forces fluctuate, there are several factors that have to be taken into consideration such as variation in the rate of penetration, effect of the coolant, area of contact between chips and the drill as well as heat flow etc,.The diagram in Fig. 8 reveals that vibratory drilling temperature results can be obtained by supplementing a temperature compensation of 10 to 30°C on temperature results associated with conventional drilling.

5. Conclusions

The following conclusions can be drawn from this experiment.

1) The dynamic component of cutting forces as well as tool wear during vibratory drilling are lower than those in conventional drilling and as a result the chisel and face temperature near the margin are lower resulting in uniform cutting edge wear.

2) By inserting a sheathed thermocouple on the drill face, it is possible to measure the cutting temperature in various points of the cutting edge.

3) The cutting edge temperature when drilling conventionally was clarified using the finite element method and results were in close agreement with measured results.

4) A consideration should be given, when deriving the drill point temperature during vibratory drilling by, implementing a temperature compensation of 10 to 30°C on measured results when drilling conventionally.

Deriving finite element equations for cutting temperature in vibratory drilling is the next objective of the authors.

References

1) M. Tueda, K. Hasegawa: Transaction of the JSME, 28, 384 (1962).
2) S. Zaima, Y. Suzuki, H. Okushima and S. Yamada : Journal of Japan Institute of Light Metals, 31, 341 (1981).
3) K. Okushima, Y. Itagaki : Journal of the Japan Society of Precision Engineering, 36, 1 (1970).
4) K. Adachi, K. Ogawa, N. Arai, H. Igaki : Journal of Japan Institute of Light Metals, Vol.40, No. 2, 88 (1990).
5) K. Adachi, K. Ogawa. N. Arai, K. Okita, R. Niba : Bull. Japan Soc. of Engg., Vol.24, No.3, 200 (1990).
6) K. Ogawa, K. Adachi, K. Sakurai, R. Niba, Y. Takashima : Bull. of Univ. of Osaka Prefecture, Vol.39, No.1, 95 (1990).
7) K. Adachi, K. Ogawa, N. Arai, H. Igaki : Journal of Japan Institute of Light Metals, Vol.40, No. 3, 171 (1990).
8) N. Arai, K. Adachi, M. Nakamura, K. Ogawa : Proceedings of The 3rd Sino-Japan Conference on Ultraprecision Machining, Cll-01 (1990).
9) M. Yagawa, A FEM Guide for Flow and Head Conduction, Baifukan, 223 (1983).